RPE | Radiation Physics & Engineering
A Peer-Reviewed Journal
Published by K.N. Toosi University of Technology
http://rpe.kntu.ac.ir
Research Article

Radiation Physics and Engineering 2025; 6(1):65–73

Investigation of neutron dose and secondary cancer risk in pelvic and brain radiotherapy with a high-energy LINAC

Najmeh Mohammadi*
Sahand University of Technology, Tabriz, Iran

HIGHLIGHTS

- The secondary cancer risk for patients undergoing brain and pelvic radiotherapy with high-energy LINAC.
- The MCNPX2.6 code was used for the 15 MV Primus Siemens LINAC's head simulation and dose calculations.
- The neutron equivalent dose was greater for tissues/organs located near the skin compared to that of photon.
- The neutron effective dose for the pelvic and brain treatment were 0.20 and 0.26 mSv.Gy^{-1}, respectively.
- The neutron equivalent dose distribution was unfluctuating in the whole body and independent of the type of treatment.

ABSTRACT

This work aimed to assess the secondary cancer risk for patients undergoing brain and pelvic radiotherapy with high-energy linear accelerators (LINAC). Photoneutrons are produced in the LINAC's head when operating above 7 MeV and are not considered in radiotherapy treatment planning. The MCNPX2.6 Monte Carlo code was used for LINAC's head simulation. The photon and neutron doses were calculated in tissues/organs of an International Commission on Radiological Protection (ICRP) male reference voxel phantom undergoing pelvic and brain radiotherapy. The results indicated that the neutron equivalent dose was higher for tissues/organs located close to skin and, contrary to the photon equivalent dose, did not decrease sharply for tissues/organs outside of the irradiation field. Notably, neutron equivalent dose distribution was almost homogenous in whole body and did not depend on the treatment type and location of target organ. Therefore, an undesirable dose was received by healthy tissues/organs, leading to an increase in secondary cancer risk. Based on the obtained results, the neutron effective dose for the pelvic and brain treatment were 0.20 and 0.26 mSv.Gy^{-1}, respectively. The results also indicated that maximum secondary cancer risk due to neutrons was for colon (0.026%) in the pelvic treatment, while in brain treatment, it belongs to stomach (0.036%) for a delivered dose of 70 Gy. It is recommended that a mean neutron effective dose value of 0.23 mSv.Gy^{-1} can be considered in brain and pelvic treatment planning for evaluating the secondary cancer risk of high-energy LINAC radiotherapy.

KEYWORDS

Neutron Dosimetry
High-energy LINAC
Monte Carlo simulation
Voxel phantom
Secondary cancer risk

HISTORY

Received: 12 June 2024
Revised: 13 September 2024
Accepted: 7 October 2024
Published: Winter 2025

1 Introduction

High-energy linear accelerators (LINACs) are used frequently to treat deep tumors. Although the goal of radiotherapy is to deliver the treatment dose to the gross tumor volume (GTV), secondary neutrons are also generated, depositing their energies in the patient's body. These neutrons are produced in the LINAC's head when operating above 7 MeV. Because photons have an energy threshold for photoneutron interactions with heavy materials constructing the LINAC's head. Nevertheless, neutron doses are not considered in routine treatment planning procedures, whereas these particles have high relative biologic effectiveness (RBE) and may increase the secondary cancer risk to normal tissues/organs (Kry et al., 2009; Sánchez-Doblado et al., 2012). Thus, considering the doses of secondary neutrons in the treatment plans becomes a noteworthy subject for researchers. Hence, many researchers are concerned about distinguishing the effects of different neutron doses on healthy tissues and organs. In this context neutron spectrum measurements were performed via various neutron spectrometry meth-

*Corresponding author: n_mohammadi@sut.ac.ir

https://doi.org/10.22034/rpe.2024.462635.1197

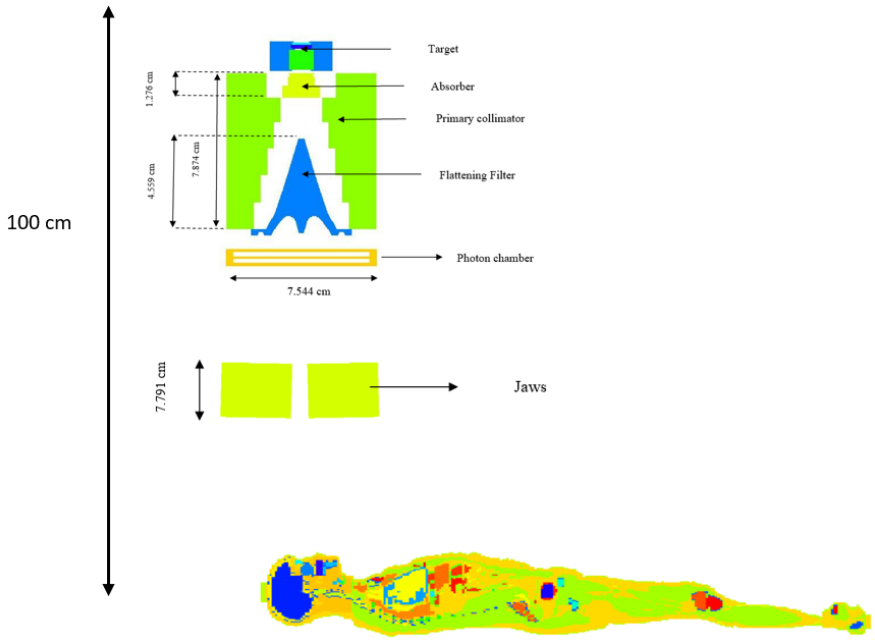

Figure 1: The view of the voxel phantom and LINAC's head, including target (Au), absorber (Al), primary collimator (W), flattening filter (SST), photon chamber (Al_2O_3), and jaws (W), in the brain treatment for AP irradiation (not to scale).

ods such as gold foil-based Bonner sphere sets (Mohammadi et al., 2015a), thermoluminescent dosimeters (TLD) (Mukherjee et al., 2005; Hsu et al., 2010), bubble detectors (ICRP, 2007; Ongaro et al., 2000), and CR-39 films (Rajesh et al., 2020). Evaluation of the received dose to the normal tissues outside the treatment field is essential because it can be used for a more accurate estimation of the risk of secondary tumors induced by radiation. In this regard, neutron dosimetry of patients undergoing radiotherapy has been also distinguished for various models and operating energies of the LINAC. However, many reported studies were limited and confined to the simplified model of the body (Alem-Bezoubiri et al., 2014; Barquero et al., 2005; Ghiasi and Mesbahi, 2010; Mohammadi et al., 2014). Some studies were done to investigate the neutron dose during the pelvic treatment (Sánchez-Nieto et al., 2017; Stathakis et al., 2007; Thalhofer et al., 2014; Bezak et al., 2017). Stathakis et al. showed that the risk of secondary malignancies from the application of IMRT was more than conventional radiotherapy. They also concluded that the whole-body dose equivalent was affected by collimator rotation, field size, and the energy of the photon beam (Stathakis et al., 2007). In this regard, the risk of secondary cancer for a 70 Gy pelvic treatment delivered by the 18 MV Siemens, 15 MV Varian, and 18 MV Varian beams was found 1.1, 1.1, and 2.0%, respectively (Chibani and Ma, 2003).

Nevertheless, it is a bit challenging to evaluate the neutron dose for other treatment areas. This is the question that is the neutron dose distribution depends on the treatment area or not. To address this problem, the present work aimed to evaluate the equivalent and effective doses of neutrons and photons received by patients during two different treatments of pelvic and brain with a 15 MV Siemens Primus LINAC that has not been reported until now. Additionally, in these treatments, the risk of fatal cancer has been estimated in different organs. It was proposed to investigate the effect of the treatment area on the neutron dose distribution on the body using the Monte Carlo MCNPX code version 2.6.

2 Materials and Methods

2.1 Voxel phantom

To evaluate the energy deposition of neutrons and photons in the body tissues/organs of a patient undergoing radiotherapy, the ICRP reference adult male voxel phantom was employed as the detailed human body model (ICRP, 2009). The voxel phantoms were developed based on computed tomography (CT) images of a human body, providing a much more realistic human anatomy. The ICRP reference adult male phantom was constructed from the tomographic dataset belonging to a male with a height and mass of 176 cm and 70 kg, respectively. It included 122 tissues/organs, and the voxel's dimensions were 2.137 mm × 2.137 mm × 8 mm.

2.2 Treatment plan simulation

The 15 MV Primus Siemens LINAC's head was simulated in detail using the MCNPX2.6 code developed by Los Alamos National Laboratory (Pelowitz et al., 2005). This simulation has been validated in a previous study (Mohammadi et al., 2015b). The pelvic and brain treatments were chosen based on the data given from the Reza Radiation Oncology Center (RROC), in which the prostate and brain are the target of treatment, respectively. Each intended treatment plan was made using the four-field box technique. For the pelvic treatment plan, the irradiation fields were 16×20.6 cm^2 for both anterior-posterior

Table 1: Photon equivalent dose ($mSv.Gy^{-1}$) of various tissues/organs during the pelvic and brain treatment.

	AP		PA		LLAT		RLAT	
	Pelvic	Brain	Pelvic	Brain	Pelvic	Brain	Pelvic	Brain
Adrenals	2.58	6.76	3.42	14.12	3.14	9.54	3.17	1.71
ET1, ET2	11.46	143.46	6.35	117.22	12.25	27.50	12.72	320.46
Brain	7.87	1000.00	8.60	1000.00	11.81	1000.00	11.38	1000.00
Colon	85.11	27.05	93.14	12.75	60.43	22.89	66.53	7.18
Testes	494.76	26.86	559.43	11.53	244.73	16.43	235.41	6.81
Liver	2.68	12.35	2.70	5.96	3.36	16.95	2.37	1.36
Lungs	2.99	5.00	3.04	4.12	3.14	4.48	3.73	2.92
Esophagus wall	4.90	8.73	4.01	6.61	3.75	7.48	4.74	6.91
Salivary glands	11.34	15.55	9.27	24.11	11.04	36.81	11.56	747.25
Skin	59.09	29.10	61.64	36.28	47.81	31.83	47.59	41.99
Stomach	2.96	15.93	2.69	4.69	2.48	5.90	3.29	2.94
Thyroid	10.83	14.90	5.89	10.67	7.16	15.38	8.18	14.18
Urinary bladder wall	1108.95	31.58	906.53	18.62	849.75	24.06	865.52	8.70
Gall bladder wall	3.31	17.80	3.36	7.28	3.78	22.50	2.96	1.33
Small intestine wall	132.57	28.30	136.14	14.84	111.98	22.23	111.98	8.51
Heart	2.67	5.58	2.09	3.27	2.05	3.57	2.83	2.36
Kidney	3.67	12.44	4.47	16.22	4.79	16.49	4.71	3.73
Lymphatic nodes	177.60	18.74	155.74	11.53	99.17	15.26	98.64	23.60
Muscle	103.98	19.29	104.47	16.27	175.81	18.27	178.06	24.84
Pancreas	3.75	18.40	3.92	9.05	3.82	15.14	3.79	2.14
Prostate	1000.00	28.31	1000.00	18.08	1000.00	21.52	1000.00	7.76
Spleen	1.89	5.16	2.79	9.27	1.98	2.52	3.46	2.72
Thymus	9.02	10.96	2.92	7.08	5.32	7.65	6.93	5.81
Eye lenses	11.82	664.82	6.19	856.40	9.92	17.78	11.76	24.50
rectum	866.41	22.66	1169.41	23.30	923.67	25.02	887.00	7.87
Active marrow	114.71	39.86	113.96	45.47	201.96	27.09	204.47	74.45
Bone surface	64.91	61.18	64.72	73.02	155.88	34.35	157.14	119.75

(AP) and posterior-anterior (PA) applications, with monitor units (MUs) of 51 and 48, respectively. For left-lateral (LLAT) and right-lateral (RLAT) irradiation, the fields were 10×20.6 cm^2 with 63 MUs (1 MU = 1 cGy for an isocenter and reference field of 10×10 cm^2). For the brain treatment plan, the irradiation fields were 5×5 cm^2 with the same MUs of all beam orientations for the pelvic treatment. In the considered treatments, the prostate and brain were set as the respective isocenters. The objective of the treatment plan was to deliver 200 cGy to the GTV in the prostate and brain. The view of the LINAC's head and the phantom are shown in Fig. 1 for the brain treatment.

2.3 Monte Carlo Simulation

In this study, the radiation transport simulation was carried out with the MCNPX2.6 code. In the input file, the electron was defined as the source, which was incident on the gold target on the LINAC's head. In All simulations, the number of 2×10^9 electron histories were traced. Photoneutron production was considered by applying the PHY card. Two runs were done separately for photon and photoneutron calculations. For photon dose calculations, the energy cutoff for electrons and photons was assumed as 0.5 and 0.01 MeV, respectively. However, for the photoneutron dose calculations, these cutoff energies were set 7 MeV below the threshold of photonuclear interactions.

Photons and photoneutrons were transported, and the absorbed doses were calculated in the different tissues/organs using the F6 tally. For this determination, the output of the F6 tally was multiplied by 160 to obtain the absorbed dose in terms of pGy. The protection quantity of equivalent dose in tissues/organs (H_T) was estimated based on the ICRP 103 definition (ICRP, 2007):

$$H_T = w_R D_T \tag{1}$$

where D_T is the absorbed dose and w_R is the radiation weighting factor for radiation type R. As defined in ICRP 103, this factor is equal to 1 for photons, while for neutrons, it depends on their energy. The average of WR value was calculated for each orientation upper the phantom, using the DE and DF cards in MCNP input file, and was found to be 15.45, 13.89, 16.06, and 15.48 for the AP, PA, LLAT, and RLAT irradiations, respectively. The effective dose (E), as another protection quantity, was evaluated using the following formula:

$$D_T = \sum_T w_T H_T \tag{2}$$

where w_T is the tissue weighting factor given in ICRP 103. Next the neutron equivalent doses were estimated, the risk of secondary cancer was calculated using the nominal fatality probability coefficients for individual tissues/organs given in Report 116 of the National Council of Radiation Protection and Measurements (NCRP) (NCRP, 1993). These coefficients refer to organs including the urinary bladder, bone marrow, bone surface, breast, colon, liver,

Table 2: Neutron equivalent dose (mSv.Gy^{-1}) of various tissues/organs during the brain treatment.

	AP		PA		LLAT		RLAT	
	Neutron equivalent dose	Relative error (%)	Neutron equivalent dose	Relative error (%)	Neutron equivalent dose	Relative error (%)	Neutron equivalent dose	Relative error (%)
Femora	0.22	4.00	0.10	3.00	0.14	5.00	0.06	4.00
Pelvic	0.27	4.00	0.16	4.00	0.17	6.00	0.06	6.00
Ribs	0.28	3.00	0.28	2.00	0.27	3.00	0.10	3.00
Sacrum	0.06	6.00	0.41	4.00	0.12	7.00	0.04	8.00
Sternum	1.13	6.00	0.08	12.00	0.19	12.00	0.09	13.00
Cartilage	0.34	5.00	0.25	3.00	0.24	6.00	0.11	6.00
Brain	0.49	5.00	0.49	4.00	0.84	4.00	0.31	4.00
Gall bladder wall	0.40	10.00	0.07	7.00	0.40	8.00	0.01	8.00
Stomach wall	0.58	6.00	0.09	8.00	0.05	9.00	0.15	7.00
Small intestine wall	0.39	3.00	0.10	3.00	0.15	5.00	0.09	5.00
Rectum wall	0.08	11.00	0.28	10.00	0.08	10.00	0.03	27.00
Colon	0.46	4.00	0.11	4.00	0.30	5.00	0.18	5.00
Heart wall	0.51	5.00	0.12	4.00	0.09	7.00	0.06	5.00
Kidneys	0.10	7.00	0.37	5.00	0.20	7.00	0.07	7.00
Liver	0.42	4.00	0.14	5.00	0.45	4.00	0.02	6.00
Lungs-tissue	0.54	3.00	0.28	3.00	0.19	4.00	0.08	4.00
Lymphatic nodes	0.57	3.00	0.21	3.00	0.21	4.00	0.11	4.00
Muscle tissue	0.42	1.00	0.37	1.00	0.37	1.00	0.15	1.00
Esophagus wall	0.42	9.00	0.22	5.00	0.17	9.00	0.07	7.00
Pancreas	0.27	7.00	0.08	7.00	0.10	10.00	0.03	7.00
Prostate	0.18	14.00	0.09	9.00	0.06	22.00	0.02	11.00
Skin	0.14	1.00	0.11	1.00	0.14	1.00	0.06	1.00
Spinal cord	0.19	7.00	0.55	5.00	0.24	6.00	0.11	7.00
Spleen	0.11	8.00	0.44	7.00	0.06	13.00	0.11	7.00
Teeth	0.67	7.00	0.11	7.00	0.43	6.00	0.18	6.00
Testes	0.55	12.00	0.03	19.00	0.04	14.00	0.03	38.00
Ureters	0.17	5.00	0.15	6.00	0.11	7.00	0.04	9.00
Urinary bladder wall	0.35	8.00	0.09	7.00	0.06	8.00	0.03	8.00
Active marrow	0.33	2.00	0.35	1.00	0.29	2.00	0.11	2.00
Bone surface	0.30	2.00	0.24	2.00	0.30	2.00	0.11	2.00

lung, esophagus, gonads, skin, stomach, thyroid, brain, salivary glands and the remainder organs. The remainder organs were considered as adrenals, Extrathoracic (ET), gall bladder, heart, kidneys, lymphatic nodes, muscle, oral mucosa, pancreas, prostate, small intestine, spleen, thymus, and uterus.

3 Results

3.1 Photon equivalent dose

The photon equivalent doses of various tissues/organs were calculated per 1 Gy absorbed by the prostate and brain in the treatment plans across the four orientations, the results of which are presented in Table 1. The relative statistical uncertainty of these calculations was below 3%. Results showed that organs outside the irradiation field received lower doses than those within the irradiation field. Specifically, organs such as the prostate, testes, urinary bladder wall, and rectum, inside the irradiation field and near the isocenter, received the highest photon equivalent doses about 1000 mSv.Gy^{-1} in all angles for the pelvic treatment. For the brain treatment, the brain and eye lenses received the most prominent photon equivalent doses. Also, the photon equivalent dose was highly dependent on the beam direction due to photon interaction with tissue composition. For instance, liver in brain treatment received highest and lowest photon dose in LLAT and RLAT orientations, respectively with 91.98% relative difference. In both treatment plans, the photon equivalent doses of organs far from the treatment field were lower by a factor of 0.001 relative to those near the isocenter or GTV. It is evident that with increasing distance between tissues/organs and the treatment area, the photon equivalent dose fell; this pattern was seen in both treatment plans.

3.2 Neutron equivalent dose

The neutron equivalent doses of various tissues/organs were estimated for four gantry angles per 1 Gy absorbed dose by the prostate and brain in the pelvic and brain treatments plans. These values, with their relative statistical uncertainties, are given in Tables 2 and 3. In these tables, results with their relative uncertainties lower than 10% were reported.

According to the obtained results, the neutron equivalent dose depended on the irradiation orientation. For instance, in the pelvic treatment, the neutron equivalent dose for the small intestine wall was 0.3, 0.08, 0.08,

Table 3: Neutron equivalent dose (mSv.Gy^{-1}) of various tissues/organs during the prostate treatment.

	AP		PA		LLAT		RLAT	
	Neutron equivalent dose	Relative error (%)	Neutron equivalent dose	Relative error (%)	Neutron equivalent dose	Relative error (%)	Neutron equivalent dose	Relative error (%)
Femora	0.19	3.00	0.12	3.00	0.2	3.00	0.22	3.00
Pelvic	0.22	3.00	0.16	3.00	0.13	4.00	0.13	3.00
Ribs	0.09	3.00	0.14	2.00	0.14	3.00	0.14	3.00
Sacrum	0.07	5.00	0.37	4.00	0.06	7.00	0.06	7.00
Sternum	0.40	7.00	0.03	12.00	0.05	15.00	0.05	11.00
Cartilage	0.22	4.00	0.2	3.00	0.14	5.00	0.14	4.00
Brain	0.10	5.00	0.14	5.00	0.21	5.00	0.17	5.00
Gall bladder wall	0.13	7.00	0.04	7.00	0.16	9.00	0.02	10.00
Stomach wall	0.21	6.00	0.05	7.00	0.02	7.00	0.18	6.00
Small intestine wall	0.30	3.00	0.08	3.00	0.08	5.00	0.15	4.00
Rectum wall	0.12	7.00	0.56	8.00	0.06	7.00	0.07	12.00
Colon	0.27	3.00	0.12	4.00	0.15	5.00	0.23	4.00
Heart wall	0.13	5.00	0.06	5.00	0.04	6.00	0.09	6.00
Kidneys	0.04	6.00	0.23	5.00	0.13	7.00	0.16	7.00
Liver	0.13	5.00	0.08	5.00	0.24	4.00	0.03	7.00
Lungs-tissue	0.13	4.00	0.15	3.00	0.09	4.00	0.10	4.00
Lymphatic nodes	0.31	3.00	0.15	3.00	0.10	5.00	0.13	3.00
Muscle tissue	0.27	1.00	0.29	1.00	0.26	1.00	0.26	1.00
Esophagus wall	0.12	8.00	0.09	6.00	0.04	7.00	0.05	8.00
Pancreas	0.11	7.00	0.05	7.00	0.04	6.00	0.05	7.00
Prostate	0.31	8.00	0.2	7.00	0.05	6.00	0.06	9.00
Skin	0.07	1.00	0.08	1.00	0.08	1.00	0.08	1.00
Spinal cord	0.07	7.00	0.25	6.00	0.06	7.00	0.06	6.00
Spleen	0.04	8.00	0.21	7.00	0.03	16.00	0.33	7.00
Teeth	0.22	6.00	0.03	6.00	0.17	6.00	0.18	9.00
Testes	0.78	9.00	0.10	9.00	0.05	9.00	0.08	18.00
Ureters	0.17	5.00	0.12	5.00	0.06	6.00	0.07	5.00
Urinary bladder wall	0.49	5.00	0.14	5.00	0.07	9.00	0.07	6.00
Active marrow	0.15	2.00	0.20	2.00	0.14	2.00	0.14	2.00
Bone surface	0.15	1.00	0.15	1.00	0.16	2.00	0.16	2.00

and 0.15 mSv.Gy^{-1} for AP, PA, LLAT, and RLAT, respectively. These values were 0.39, 0.10, 0.15, and 0.09 mSv.Gy^{-1} for brain treatment.

In the brain treatment, the neutron equivalent doses at AP orientation for the stomach, heart wall, and lymphatic nodes, outside of the irradiation field, were 0.58, 0.51, and 0.57 mSv.Gy^{-1}, respectively which were larger than of brain value (0.49 mSv.Gy^{-1}). In the pelvic treatment, the neutron equivalent doses for the sternum, testes, and urinary bladder wall, which were out-field, were 0.45, 0.78, and 0.49 mSv.Gy^{-1}, respectively greater than of prostate amount (0.31 mSv.Gy^{-1}).

The neutron and photon equivalent doses in the AP direction were compared in Figs. 2 and 3 for the pelvic and brain treatments, respectively. It can be seen that the neutron equivalent dose for the brain treatment varied in the range of 0.06 to 1 mSv.Gy^{-1}. In contrast, the most significant changes occurred in the photon equivalent dose values, such that they ranged from 5 to 1000 mSv.Gy^{-1}. A similar pattern was observed for pelvic treatment. There were remarkable differences in the neutron and photon equivalent doses belonging to organs inside and outside the treatment field.

The neutron equivalent dose of various tissues/organs in each irradiation orientation was multiplied by its MU, and the total neutron equivalent dose for both treatment plans was calculated. These outcomes were plotted in Fig. 4. According to this graph, the brain received the greatest neutron equivalent doses because it was closer to the skin than the prostate, testes, and urinary bladder, which were located in the depth of the body. Except for the brain, the neutron equivalent dose values were in the same range for the remaining organs and tissues. It can be implied that, regardless of the treatment area, the unwanted neutron dose deposited to the normal tissues was the same for both treatment plans.

For two treatment plans, the effective dose was also calculated per 1 Gy absorbed dose in the target organ of the prostate and brain. According to our calculations, the effective neutron dose for the pelvic and brain treatment plans were 0.20 and 0.26 mSv.Gy^{-1}, respectively. This outcome reflected the conclusion that in treatments for pelvic and brain regions, it can be stated that proximately the neutron dose was independent of the treatment area. Additionally, considering Fig. 4, the equivalent doses vary, while the total effective dose for the whole body is approximately the same.

It should be noted that these organs were outside of the treatment area but had the highest risks. Overall, appropriate preparations are proposed to reduce the destructive

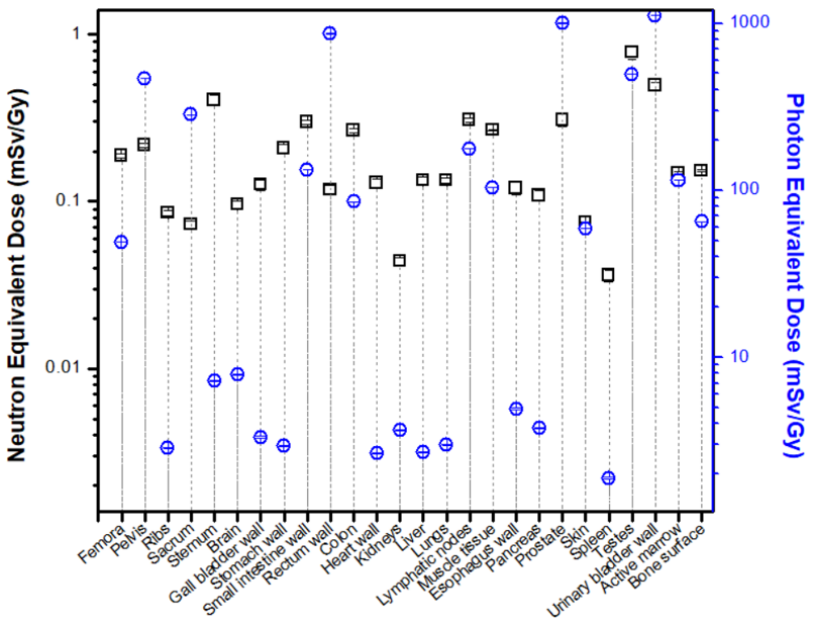

Figure 2: Copmarison of the neutron and photon equivalent dose in AP for the pelvic treatment.

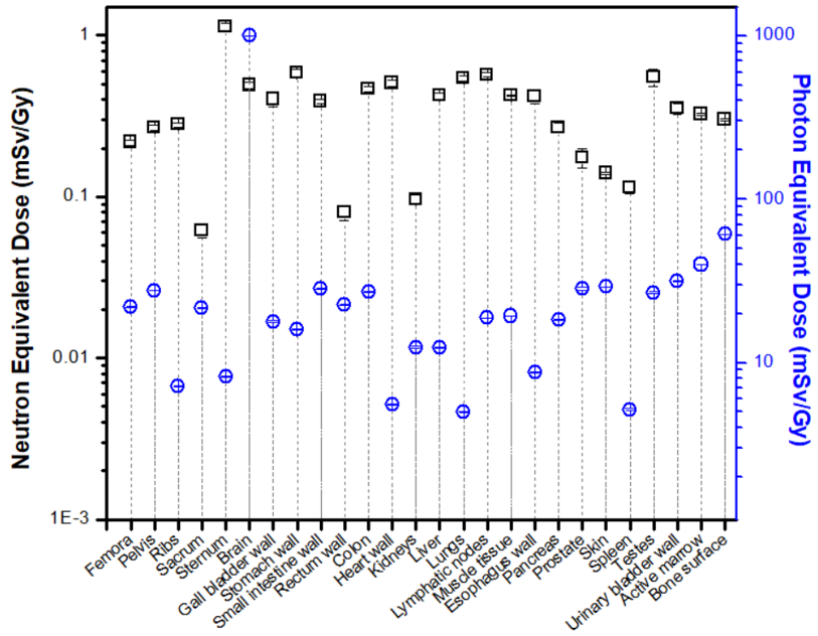

Figure 3: Copmarison of the neutron and photon equivalent dose in AP for the brain treatment.

effects of neutrons during radiotherapy.

3.3 Secondary cancer risk

To evaluate the secondary cancer risk induced by neutrons as a long-term medical consequence of radiotherapy with high-energy LINACs, a 70 Gy treatment dose was considered. For determining the risk values, the total neutron equivalent doses were multiplied by the coefficients of fatal risk given in NCRP Report No. 116. The calculated probabilities of secondary cancer risk from neutrons for vital organs are given in Table 4.

Table 4: Secondary cancer risk due to neutrons for delivered dose of 70 Gy in %.

	Pelvic treatment	Brain treatment
Bladder	0.010	0.004
Bone marrow	0.012	0.020
Bone surface	0.001	0.002
Beast	0.014	0.024
Esophagus	0.003	0.010
Colon	0.026	0.035
Liver	0.003	0.006
Lung	0.015	0.035
Gonads	0.004	0.002
Skin	0.0003	0.0004
Stomach	0.019	0.036
Thyroid	0.001	0.006
Reminder	0.097	0.146

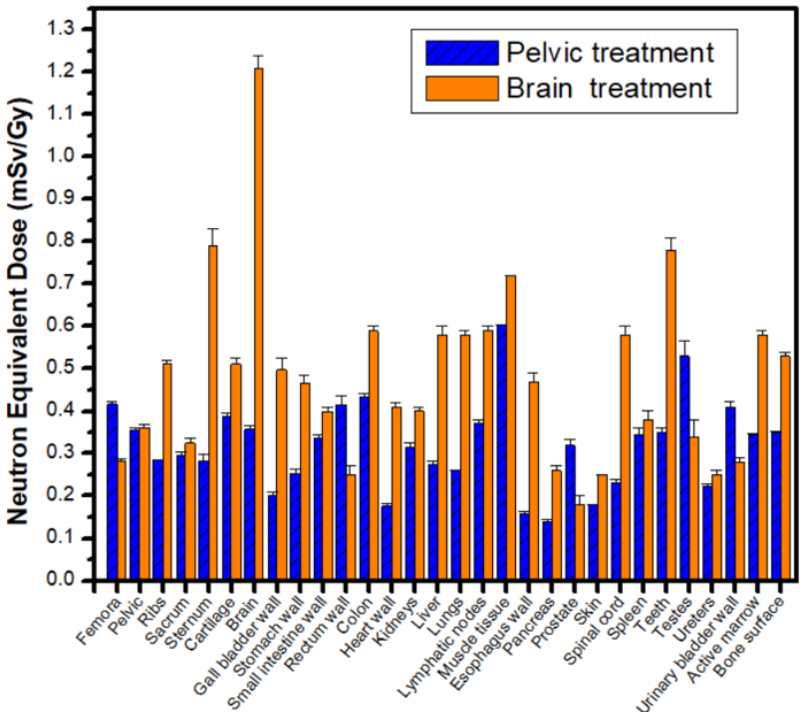

Figure 4: Total neutron equivalent dose for the pelvic and brain treatment.

4 Discussion

The calculated neutron equivalent dose of some organs of a patient during the pelvic treatment was compared with the values reported by Howell et al. (Howell et al., 2006). They measured neutron fluence in the Alderson Radiation Therapy (ART) Phantom irradiated with 15 MV Varian 23EX LINAC and neutron dose equivalent was calculated using ICRP74 quality conversion factors. Based on the obtained results, the neutron equivalent doses of the urinary bladder, colon, stomach, and liver were 0.41, 0.43, 0.25, and 0.27 mSv.Gy^{-1}, respectively; these values can be compared with those reported by Howell et al. for 15 MV Varian 23EX LINAC, which were 0.2, 0.13, 0.05, and 0.13 mSv.Gy^{-1}, respectively. These quantities were also calculated 0.70, 0.48, 0.81, and 0.58 mSv.Gy^{-1}, respectively in female phantom of Medical Internal Radiation Dose (MIRD) undergoing pelvic radiotherapy in 18 MV Varian Clinac linac (Chegeni et al., 2018). It can be seen that the reported values are comparable with our results in terms of order magnitude. However, the existing deviations are due to the differences between the models and energy of LINACs used in these studies.

It can be seen that the photon equivalent dose was strongly lower for organs outside the treatment field. It is clear from the data provided that the neutron equivalent dose distribution was relatively uniform for all tissues/organs, though organs close to the skin received greater neutron equivalent doses. This means that the normal tissues/organs outside of the irradiation field received an undesirable dose of neutrons, which is probably due to particle scattering from the LINAC's head components, room walls, and floor.

The results showed that neutron equivalent dose decreased strongly with increasing the distance from body surface. This reduction can be explained through the reduction of elastic neutron-hydrogen collisions with decreasing neutron energy in depth (Martinez-Ovalle et al., 2011). So, the energy deposition and then neutron equivalent dose were decreased. Moreover, the neutron scatting form the LINAC head has also caused to receive neutron dose by tissue/organ near the body surface. As anticipated, there is not much difference between the neutron equivalent dose for tissues/organs inside and outside of the field, though those closest to the body surface received higher neutron equivalent doses.

Considering the obtained results, the colon had the maximum secondary cancer risk (0.026%) in the pelvic treatment, while in the brain treatment the stomach had the greatest risk (0.036%). It should be noted that these organs were outside of the treatment area but had the highest risks. Overall, appropriate preparations are proposed to reduce the destructive effects of neutrons during radiotherapy.

5 Conclusions

In this work, Monte Carlo simulations were conducted to estimate the neutron equivalent dose and effective dose received by a patient undergoing pelvic and brain treatment with a 15 MV LINAC. As expected, the neutron equivalent dose was higher for tissues/organs located close to the skin and, contrary to the photon equivalent dose, did not decrease sharply for tissues/organs outside of the irradiation field. Notably, the neutron equivalent dose distribution was roughly unfluctuating in the whole body and was independent of the type of treatment. In addition, doses imparted to the patients by neutrons were such that

undesirable doses were received by the healthy tissues and organs, leading to an increase in secondary cancer risk.

According to the obtained results, it is recommended that a mean neutron effective dose value of 0.23 $mSv.Gy^{-1}$ is considered in brain and pelvic treatment plannings for evaluating the secondary cancer risk of high-energy LINAC radiotherapy.

Conflict of Interest

The authors declare no potential conflict of interest regarding the publication of this work.

References

Alem-Bezoubiri, A., Bezoubiri, F., Badreddine, A., et al. (2014). Monte Carlo estimation of photoneutrons spectra and dose equivalent around an 18 MV medical linear accelerator. *Radiation Physics and Chemistry*, 97:381–392.

Barquero, R., Edwards, T., Iniguez, M., et al. (2005). Monte Carlo simulation estimates of neutron doses to critical organs of a patient undergoing x-ray LINAC-based radiotherapy. *Medical Physics*, 32(12):3579–3588.

Bezak, E., Takam, R., Yeoh, E., et al. (2017). The risk of second primary cancers due to peripheral photon and neutron doses received during prostate cancer external beam radiation therapy. *Physica Medica*, 42:253–258.

Chegeni, N., Karimi, A. H., Jabbari, I., et al. (2018). Photoneutron dose estimation in GRID therapy using an anthropomorphic phantom: A Monte Carlo study. *Journal of Medical Signals & Sensors*, 8(3):175–183.

Chibani, O. and Ma, C.-M. C. (2003). Photonuclear dose calculations for high-energy photon beams from Siemens and Varian linacs. *Medical Physics*, 30(8):1990–2000.

Ghiasi, H. and Mesbahi, A. (2010). Monte Carlo characterization of photoneutrons in the radiation therapy with high energy photons: a Comparison between simplified and full Monte Carlo models.

Howell, R. M., Hertel, N. E., Wang, Z., et al. (2006). Calculation of effective dose from measurements of secondary neutron spectra and scattered photon dose from dynamic MLC IMRT for, and beam energies. *Medical Physics*, 33(2):360–368.

Hsu, F.-Y., Chang, Y.-L., Liu, M.-T., et al. (2010). Dose estimation of the neutrons induced by the high energy medical linear accelerator using dual-TLD chips. *Radiation Measurements*, 45(3-6):739–741.

ICRP (2007). ICRP publication 103. *Ann ICRP*, 37(2.4):2.

ICRP (2009). Adult reference computational phantoms. ICRP Publication 110. *Ann. ICRP*, 39(2):1.

Kry, S. F., Howell, R. M., Salehpour, M., et al. (2009). Neutron spectra and dose equivalents calculated in tissue for high-energy radiation therapy. *Medical Physics*, 36(4):1244–1250.

Martinez-Ovalle, S., Barquero, R., Gomez-Ros, J., et al. (2011). Neutron dose equivalent and neutron spectra in tissue for clinical linacs operating at 15, 18 and 20 MV. *Radiation Protection Dosimetry*, 147(4):498–511.

Mohammadi, N., Hakimabad, H. M., and Motavalli, L. R. (2015a). Neural network unfolding of neutron spectrum measured by gold foil-based Bonner sphere. *Journal of Radioanalytical and Nuclear Chemistry*, 303:1687–1693.

Mohammadi, N., Miri-Hakimabad, H., Rafat-Motavlli, L., et al. (2015b). Neutron spectrometry and determination of neutron contamination around the 15 MV Siemens Primus LINAC. *Journal of Radioanalytical and Nuclear Chemistry*, 304:1001–1008.

Mohammadi, N., Miri-Hakimabad, S. H., and Rafat-Motavalli, L. (2014). A Monte Carlo study for photoneutron dose estimations around the high-energy linacs. *Journal of Biomedical Physics & Engineering*, 4(4):127.

Mukherjee, B., Makowski, D., and Simrock, S. (2005). Dosimetry of high-energy electron linac produced photoneutrons and the bremsstrahlung gamma-rays using TLD-500 and TLD-700 dosimeter pairs. *Nuclear Instruments and Methods in Physics Research Section A: Accelerators, Spectrometers, Detectors and Associated Equipment*, 545(3):830–841.

NCRP (1993). NCRP Report National Committee on Radiation Protection and Measurements (US). National Council on Radiation Protection and Measurements.

Ongaro, C., Zanini, A., Nastasi, U., et al. (2000). Analysis of photoneutron spectra produced in medical accelerators. *Physics in Medicine & Biology*, 45(12):L55.

Pelowitz, D. et al. (2005). Los Alamos National Laboratory report. Technical report, LA-CP-05-0369.

Rajesh, K., Raman, R. G., Musthafa, M., et al. (2020). A passive method for absolute dose evaluation of photoneutrons in radiotherapy. *International Journal of Radiation Research*, 18(1):173–178.

Sánchez-Doblado, F., Domingo, C., Gómez, F., et al. (2012). Estimation of neutron-equivalent dose in organs of patients undergoing radiotherapy by the use of a novel online digital detector. *Physics in Medicine & Biology*, 57(19):6167.

Sánchez-Nieto, B., Romero-Expósito, M., Terrón, J. A., et al. (2017). Uncomplicated and Cancer-Free Control Probability (UCFCP): a new integral approach to treatment plan optimization in photon radiation therapy. *Physica Medica*, 42:277–284.

Stathakis, S., Li, J., and Ma, C. C. (2007). Monte Carlo determination of radiation-induced cancer risks for prostate patients undergoing intensity-modulated radiation therapy. *Journal of Applied Clinical Medical Physics*, 8(4):14–27.

Thalhofer, J., Roque, H., Rebello, W., et al. (2014). Effect of external shielding for neutrons during radiotherapy for prostate cancer, considering the 2300 CD linear accelerator and voxel phantom. *Radiation Physics and Chemistry*, 95:267–270.

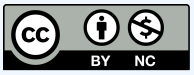

To cite this article:

Mohammadi, N. (2025). Investigation of neutron dose and secondary cancer risk in pelvic and brain radiotherapy with a high-energy LINAC. Radiation Physics and Engineering, 6(1), 65-73. doi: 10.22034/rpe.2024.462635.1197

DOI: 10.22034/rpe.2024.462635.1197

To link to this article: https://doi.org/10.22034/rpe.2024.462635.1197